Journal of Marine Science and Technology

Volume 22 | Issue 4 Article 12

OPTIMIZATION OF ELECTRICAL DISCHARGE MACHINING PARAMETERS FOR NITI SHAPE MEMORY ALLOY BY USING THE TAGUCHI METHOD

Saeed Daneshmand
Department of Mechanical Engineering, Majlesi Branch, Islamic Azad University, Isfahan, Ira,
s.daneshmand@iaumajlesi.ac.ir

Ehsan Farahmand Kahrizi
Department of Mechanical Engineering, Majlesi Branch, Islamic Azad University, Isfahan, Ira

Ali Akbar LotfiNeyestanak
Department of Mechanical Engineering,Yadegar -e- Imam Khomeini (RAH) Branch, Islamic Azad University, Tehran, Iran

Vahid Monfared
Department of Mechanical Engineering, Zanjan Branch, Islamic Azad University, Zanjan, Iran.

Journal of Marine Science and Technology, Vol. 22, No. 4, pp. 506-512 (2014)
DOI: 10.6119/JMST-013-0624-1

OPTIMIZATION OF ELECTRICAL DISCHARGE MACHINING PARAMETERS FOR NITI SHAPE MEMORY ALLOY BY USING THE TAGUCHI METHOD

Saeed Daneshmand[1], Ehsan Farahmand Kahrizi[1], Ali Akbar LotfiNeyestanak[2], and Vahid Monfared[3]

Key words: electrical discharge machining, optimization, Taguchi method, material removal rate, surface roughness, nickel titanium alloy.

ABSTRACT

Electrical discharge machining (EDM) is among the most essential nontraditional machining processes. Material removal rate (MRR) and surface roughness are the two main parameters applied in this method. A desired surface roughness can be achieved at the maximal MRR by selecting the optimal input parameters. Because of the mechanical properties and hardness of shape-memory nickel titanium (NiTi) alloy, material can be removed using an EDM method. NiTi alloy is widely used in marine science and aerospace industries. Surface roughness is a critical parameter affecting the machining of this alloy. This study examined the effect the input parameters (pulse current, gap voltage, pulse on time, and pulse off time) on the output parameters (surface roughness and MRR) to determine the minimal surface roughness and maximal MRR for NiTi alloy. Accordingly, the Taguchi method and analysis of variance were employed to optimize the machining parameters. The modeling and experimental results indicate that pulse current and pulse-on time are the most critical parameters affecting MRR and surface roughness.

Paper submitted 11/03/11; revised 05/02/13; accepted 06/24/13. Author for correspondence: Saeed Daneshmand (e-mail: s.daneshmand@iaumajlesi.ac.ir).
[1] Department of Mechanical Engineering, Majlesi Branch, Islamic Azad University, Isfahan, Iran.
[2] Department of Mechanical Engineering,Yadegar -e- Imam Khomeini (RAH) Branch, Islamic Azad University, Tehran, Iran.
[3] Department of Mechanical Engineering, Zanjan Branch, Islamic Azad University, Zanjan, Iran.

I. INTRODUCTION

Electrical discharge machining (EDM), a widely used method for shaping conductive materials, can be used to remove material by creating controlled sparks between a shaped electrode and electrically conductive workpiece [3]. During this process, an electrical spark acts as a cutting tool to erode the workpiece and produce a desired shape. The metal-removal process involves applying a pulsating (ON–OFF) electrical charge with high-frequency current through the electrode and onto the workpiece, eroding the metal at a controlled rate. Dielectric fluid is flushed into the gap between the electrode and workpiece to remove small particles that are created during the process and to prevent excessive oxidation of both the workpiece surface and electrode [11, 13]. Shape memory alloys (SMAs) exhibit unique thermal and mechanical properties that have been studied extensively for more than 50 years. Moreover, demand for industrial and commercial applications has increased over the last 15 to 20 years. The ability of SMAs to recover from large strains caused by thermal and mechanical loading has led to the development of numerous applications in the biomedical, oil, and aerospace industries [5, 7, 8, 14]. Marine scientists have examined the potential for using SMAs in thermally activated actuator applications [20]. For example, SMAs are used widely in free recovery, constrained recovery, actuation recovery, and super elastic recovery [21]. Shape memory materials are characterized by a unique correlation among strain, stress, and temperature based on crystallographic reversible, thermo elastic martensitic transformation. The low and high temperature phases are respectively related to martensite and austenite in steel technology. The respective temperatures at the beginning and completion of the transformation are the austenite start temperature (As) and austenite finish temperature (Af), and those during heating and cooling at the martensite start temperature (Ms) and martensite finish temperature (Mf).

Temperature-triggered transformation can be accompanied

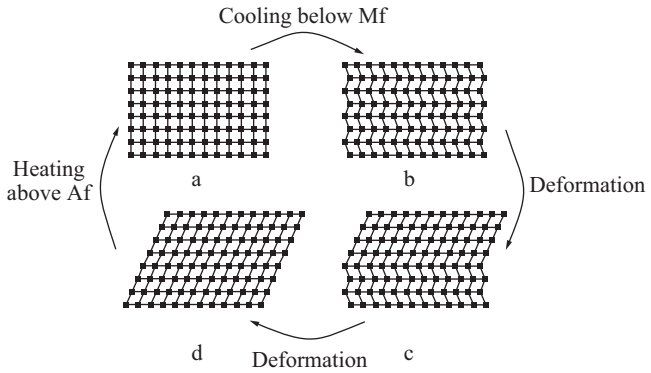

Fig. 1. Different phases of a shape memory alloy [20].

Fig. 2. EDM machine, model: 204H.

by an unusually large strain; when external forces constrain the deformation, the stress can increase markedly (i.e., capability to perform mechanical work). At temperatures above Af and below Md (the highest temperature at which stress-induced martensite forms), increased stress levels can trigger the reversible martensitic transformation. In this case, an unusually large strain accompanied by a small additional stress increase would be possible (pseudo elasticity). When unloaded, transformation and shape-change occur in the reverse direction and order. At temperatures higher than Md, plastic transformation occurs before the onset of the martensitic transformation. When martensite is deformed and heated to as, the material returns to its original shape [1]. Pseudo-plastic deformation is characterized not by gliding and generating dislocations, but by the movement of twin boundaries that reduce the number of martensitic variants. Upon cooling, the shape remains unchanged. This phenomenon is called the one-way shape memory effect, specifically because shape-change occurs only while heating the material. This effect is a natural crystallographic property of shape memory materials (Fig. 1). Strain values as high as 8% can be recovered in poly-crystalline NiTi alloys. NiTi is the most well-known SMA with near-equiatomic composition. The transformation temperature decrease sharply with increasing Ni content. The high-temperature phase (austenite) has a body-centered cubic structure, whereas the low-temperature phase (martensite) has an ordered monoclinic structure [9].

This study investigated a method for achieving a high-quality surface and high material-removal rate (MRR) while improving the dimensional accuracy and reducing the cost and tool-wear by selecting the optimal input parameters (voltage, pulse current, gap, pulse-on time, and dielectric fluid). Because of the high cost of EDM and complex physical relationship between the input and output parameters, previous studies have endeavored to model and optimize the EDM parameters [10]. Patel *et al*. used mathematical methods to study the modeling and simulation of an anode erosion model. Geat flux was assumed to follow a Gaussian distribution on the anode surface, and the stored energy was applied as a boundary condition [16]. Moreover, some studies have used artificial intelligence techniques to model machining processes. Panda and Bhoi used a neural network based on error-preprocessing to model the MRR in EDM, and developed a network model that for estimating the MRR according to the input parameters [15]. The model can also be realized using statistical methods to determine the relationship among the design variables. Petropoulos *et al*. studied the relationship between surface texture parameters and input process parameters by performing a multivariate analysis and comparing the results with the experimental results [17]. Ashish *et al*. surveyed the optimal values of input process parameters (pulse current, voltage, gap, and pulse on time) by using the Taguchi method to estimate the maximal MRR and minimal tool-wear rate for a carbon composite sample [2]. Fattouh *et al*. calculated the optimal value that could be used to reduce costs and increase production rates, by employing a response level method and improving the relationships between the input and output parameters employed during the process [6]. By contrast, the present study investigated the amount of input process parameters by using the Taguchi method separately and simultaneously to achieve the maximal MRR and minimal surface roughness. Moreover, the effect that the parameters exerted on the surface roughness and MRR was determined by performing an analysis of variance (ANOVA). The pulse current, voltage, gap, and pulse on–off time were the input parameters, and the MRR and surface roughness were the output parameters. A mathematical model was eventually devised to estimate the MRR and surface roughness by applying regression equations.

II. EQUIPMENT AND TEST METHODS

The EDM specimens were created using a 204-H die-sinking EDM machine (Tehran EKRAM Co., Iran; Fig. 2). In this study, NiTi60 was adopted as the workpiece material, which had a density of 6.45 gr/cm^3. The samples were cut into plate forms with dimensions of 40 mm $\times$ 50 mm from raw materials, and then ground using wire electro discharge machining (WEDM). Table 1 lists the mechanical and physical properties of NiTi60.

Table 1. Mechanical and physical properties of NiTi60.

density	6.45 G/cc
tensile strength, ultimate	850 MPa
tensile strength, yield	560 MPa
modulus of elasticity	75.0 GPa
poisson's ratio	0.300
electrical resistivity	0.0000820 Ohm-cm
thermal conductivity	10.0 W/m-k
melting point	1240-1310°C
nickel, Ni	55.0%
titanium, Ti	45.0%

The tools used in this study were composed of brass with dimensions of φ = 8 mm × 40 mm. In addition, machining and abrasive grinding were performed on the tool surface to prevent the workpiece and tools from becoming nonparallel, because of the effect of tool surface roughness on the workpiece surface. All of the tests were performed within 1 day to prevent changes to the test conditions. Deionized water with an EC of less than 1 μS was used to improve the accuracy test and prevent the effect caused by oil-based dielectrics combined with the workpiece surface. In addition, a spray-washing system was used for constant spraying throughout the experiments. An A&D GR-300 lab balance of 0.1 mg (i.e., it reduced uncertainty in the weight measurements with a resolution of 0.1 mg (insert a closing bracket after 0.1 mg), and was used to measure the volume of the material removed from the workpiece and tools. A Mahr roughness tester (M300-RDI8) was used to determine the workpiece surface roughness.

III. DESIGN OF EXPERIMENTS

Among the various effective factors influencing a test, some are more crucial than others. The experimental design provided information regarding the effective parameters for a response. Various parameters were selected for further investigation, and the control input parameters were changed systematically; the parameter effects on the output parameters have already been discussed and evaluated in a previous study [12]. The input parameters included the pulse–on time, pulse-off time, voltage, and discharge current, and the output parameters comprised the surface roughness and MRR. Taguchi's experimental design method was used to design and analyze the machining parameters. An L9 orthogonal array and the repetitive-levels technique employing a repeated voltage level of 80 were used to optimize the number of experiments and generalize the results to all of the investigated levels, because the EDM machine used in this study had only two voltage levels. In this study, nine trials were conducted, and the number of factors was four [18]. The current, voltage, and pulse-on and -off times were the factors or input parameters used in this experiment. The voltage factor had two levels, and the current as well as the pulse-on and -off times had three levels. The current discharge value oscillated between 10 and 20 A, because the MRR was negligible below the lower limit, and an acceptable level was not achieved for the pulse current exceeding the upper limit. According to the capability of the machine, the applied voltages were 80 and 250 V. Moreover, 35 μs, 50 μs, and 100 μs were used for the pulse-on time; flushing exceeding 100 μs was reduced, which affected the MRR. The pulse-off time was 30, 70, and 200 μs. Table 2 shows the design factors and selected levels for each experimental parameter. In addition, an analysis was performed using MiniTab® 16.1.1 software. Machining was executed using a fixed time, and the MRR was measured by determining the weight difference of the workpiece before and after machining. The MRR, measured in cubic millimeters per minute, was obtained using Eq. (1).

Table 2. Input parameters of EDM and designated levels.

Factors	levels		
gap voltage (V)	-	30 V	250 V
discharge current (A)	10 A	15 A	20 A
pulse duration (μs)	35 μs	50 μs	100 μs
pause duration (μs)	30 μs	70 μs	200 μs

$$MRR = \frac{(W_1 - W_2)}{\rho_w \times t} \times 10^3 \quad (1)$$

where W_1 and W_2 are the workpiece weight before and after machining, respectively, ρ_w is the density of the NiTi SMA, and t is the machining time (min). The tool wear (mm^3/min) was obtained using Eq. (2):

$$TWR = \frac{(T_1 - T_2)}{\rho_t \times t} \times 10^3 \quad (2)$$

where TWR is the tool wear rate (mm^3/min), T_1 and T_2 are the tool weight before and after machining, respectively, ρ_t is the density of the graphite tools, and t is the machining time (min). The electrode wear rate (EWR) was calculated using Eq. (3):

$$EWR = \frac{TWR}{MRR} \times 100 \quad (3)$$

where TWR is the tool wear rate (mm^3/min), MRR is the material-removal rate (mm^3/min), and EWR is the electrode wear rate (mm^3/min).

IV. CONTROL FACTORS AND SELECTING THE TAGUCHI STANDARD ORTHOGONAL ARRAY

The pulse current, voltage, pulse-on time, and pulse-off

Table 4. Design of Experiments and output parameters.

experimental design using L9 orthogonal array						
	control factors levels				output parameters	
experiment number	voltage	pulse on time	discharge current	pulse off time	surface roughness (Ra)	MRR
1	1	1	1	1	4.31800	6.0724
2	2	2	2	1	5.18067	8.6305
3	3	3	3	1	7.58733	14.9354
4	3	2	1	2	5.58267	3.8501
5	1	3	2	2	7.07167	10.6718
6	2	1	3	2	6.01367	4.7028
7	2	3	1	3	4.14033	11.4470
8	3	1	2	3	5.02767	3.1525
9	1	2	3	3	7.71433	9.9225

Table 3. Machining parameters and their levels.

experiment levels	voltage	pulse on time	discharge current	pulse off time
level 01	80	35	10	30
level 02	250	50	15	70
level 03	80	100	20	200

time were the input parameters and control factors, and the output parameters included the MRR and surface roughness. Among the input parameters, the voltage had two levels, and the other parameters had three levels. Table 3 lists the experimental input parameters.

The Taguchi orthogonal array was chosen according to the degrees of freedom (DOF) of all of the control factors. The orthogonal array was a matrix containing the input parameters with various levels; each row in the matrix represented individual experiments and various conditions. In each column, all of the levels of an input parameter were listed and repeated in a similar manner. The DOF were determined using Eq. (4).

$$1 + \text{Number of factors} \times (\text{Number of level-1}) = \text{degrees of freedom (DOF)}$$
$$1 + 4 \times (3 - 1) = \text{DOF} \quad (4)$$

According to the DOF, the L9 orthogonal array was used (Table 4). Table 4 lists the values of the surface roughness and MRR obtained by applying the orthogonal array in the nine experiments. The output results were calculated using the Taguchi analysis function in the MiniTab® 16.1.1 software, in accordance with the experimental data. Figs. 3 and 4 show the effects voltage, pulse current, pulse-on time, and pulse-off time exerted on the MRR and surface roughness of the NiTi SMA that was created using brass instruments and a deionized-water dielectric. The pulse current was the most effective parameter in achieving a reasonable MRR and surface roughness for the NiTi alloy. An increased pulse current caused an increase in spark energy; therefore, larger discharge craters formed on the workpiece surface, and the surface roughness and MRR increased.

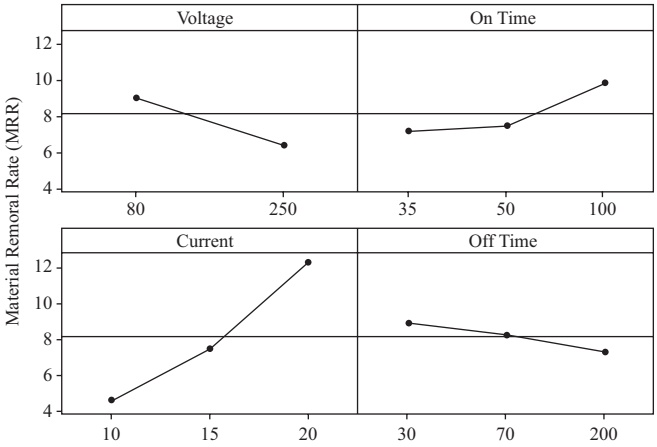

Fig. 3. Variation of material removal rate with pulse-on-time, pulse-off-time, pulse current and gap voltage.

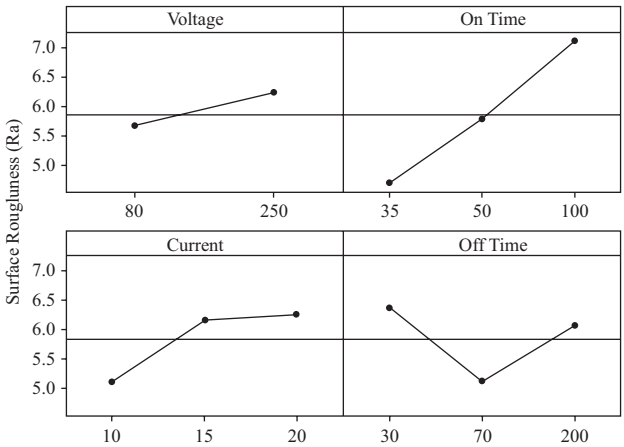

Fig. 4. Variation of surface roughness with pulse-on-time, pulse-off-time, pulse current and gap voltage.

Table 5. Analysis of variance for material removal rate.

source	DOF	SS	MS	F	P
voltage	1	13.7	13.7	0.85	0.387
pulse on time	2	13.2	6.6	0.35	0.718
discharge current	2	91.26	45.63	7.81	0.021
pulse off time	2	3.8	1.9	0.09	0.913

Table 6. Calculation error of regression equation (Eq. (5)) and experimental result.

experiment number	MRR exprimental result	MRR regression equation	error %
1	6.0724	6.0724	9.260E-4
2	8.6305	8.6306	9.124E-4
3	14.9354	14.9355	7.357E-4
4	3.8501	3.8502	**24.999E-4**
5	10.6718	10.6719	9.34E-4
6	4.7028	4.7029	9.978E-4
7	11.4470	11.4471	9.105E-4
8	3.1525	3.1525	22.401E-4
9	9.9225	9.9225	6.962E-4

V. ANALYSIS OF VARIANCE

Table 4 lists the MRR ANOVA results. At a 95% confidence level and with a *p* value of less than 0.05, the pulse current had the greatest effect on the MRR, and this effect decreased gradually for the voltage, pulse-on time, and pulse-off time. The sum of squares (SS), variance (V), DOF, the effect of each parameter (PC%), and the importance of the input parameters (F) were calculated for optimizing by applying statistical methods (Table 5). The regression equation in Eq. (5) expresses the MRR obtained using the response surface technique. Table 6 lists the relative error of this equation compared with the measured results. According to the results, the maximum error was 24.999E-4%, and the equation average error was equal to 0.0012058%, which was negligible. Therefore, the equation predicted the MRR response satisfactorily [4].

$$\begin{aligned} MRR = {} & 15.5226 - (0.00599762 * \text{'Voltage'}) \\ & - (0.198155 * \text{'On Time'}) - (1.25301 * \text{'Current'}) \\ & + (0.0581298 * \text{'Off Time'}) \\ & + (0.000357782 * \text{'On Time'}^2) \\ & + (0.0411714 * \text{'Current'}^2) \\ & - (3.12133E\text{-}4 * \text{'Off Time'}^2) \\ & + (0.0127907 * \text{'On Time'} * \text{'Current'}) \end{aligned} \quad (5)$$

According to the ANOVA results on surface roughness (Table 7), for 95% confidence levels and a *p* value smaller than 0.05, the pulse-on time was the main parameter, and the other parameters, such as the pulse-off time, pulse current, and voltage, respectively showed substantial and critical effects on the process. Eq. (6) is the regression equation used to determine the relationship between the surface roughness and the four mentioned parameters. The equation was obtained using the response surface technique. Table 8 shows a comparison of the data obtained from this equation and the experimental data, and lists the resultant error. The maximal error of this equation was 2.62998%, and the average error was 0.862313%, which could be negligible. Thus, Eq. (6) was used to obtain the surface roughness accurately.

Table 7. Analysis of variance for surface roughness.

source	DF	SS	MS	F	P
voltage	1	0.63	0.63	0.32	0.590
on time	2	8.855	4.427	4.72	0.059
current	2	2.4	1.20	0.60	0.580
off time	2	2.58	1.29	0.65	0.555

Table 8. Calculation error of regression equation (Eq. (6)) and experimental result.

experiment number	experimental result Ra	regression equation Ra	error %
1	4.31800	4.32024	0.05188
2	5.18067	5.17404	0.12791
3	7.58733	7.48394	2.42674
4	5.58267	5.44719	24.999E-4
5	7.07167	7.08094	0.13113
6	6.01367	6.03364	0.33213
7	4.14033	4.12994	0.25103
8	5.02767	4.89544	**2.62998**
9	7.71433	7.74884	0.44731

$$\begin{aligned} Ra = {} & -2.84146 + (0.00368 * \text{'Voltage'}) \\ & + (0.12329 * \text{'On Time'}) + (0.64260 * \text{'Current'}) \\ & - (0.05107 * \text{'Off Time'}) - (0.00069 * \text{'On Time'}^2) \\ & - (0.01864 * \text{'Current'}^2) + (0.00021 * \text{'Off Time'}^2) \\ & + (0.00051 * \text{'On Time'} * \text{'Current'}) \end{aligned} \quad (6)$$

VI. SIGNAL-TO-NOISE RATIO ANALYSIS BASED ON THE TAGUCHI METHOD

The analysis of signal-to-noise (S/N) ratios involved optimizing the EDM parameters by using the Taguchi method. The S/N ratio, the ratio of the desirable value of a characteristic to the undesirable value of an output characteristic, was obtained through two steps. First, the mean squared deviation

Table 9. Analysis of normalized output parameters ratio.

experiment number	estimated S/N ratio		normalized output	
	surface roughness (μm)	MRR mm^3/min	surface roughness (μm)	MRR mm^3/min
1	12.7057	15.6671	0.71597	0.66713
2	14.2877	18.7207	0.80512	0.79716
3	17.6018	**23.4843**	0.99187	**1.00000**
4	14.9368	11.7095	0.84170	0.49861
5	16.9904	20.5648	0.95742	0.87568
6	15.5828	13.4472	0.87810	0.57260
7	12.3407	21.1739	0.69541	0.90162
8	14.0273	9.9730	0.79045	0.42467
9	**17.7460**	19.9324	**1.00000**	0.84875

(MSD) of the MRR and R_a was calculated, and then the S/N ratio was assessed according to the MSD, by considering the output parameters and relevant quality indicators. Three quality indicators were used to analyze the S/N ratio:

1- A small amount of output data or factors, such as the surface roughness, was desirable, and was obtained using Eq. (7):

$$\eta_i = -10Log_{10}[\frac{1}{n}\sum\nolimits_{i=1}^{n} y^2] \quad (7)$$

where *in* is the S/N ratio at the *i*th test, *yi* is the *i*th test, and *n* is the total.

2- A large amount of the output data or factors, such as the MRR, was preferable, and was measured using Eq. (8):

$$\eta_i = -10Log_{10}[\frac{1}{n}\sum\nolimits_{i=1}^{n}(\frac{1}{y_i^2})] \quad (8)$$

3- Having a determined value for the output data or factor was desirable, and was obtained using Eq. (9).

$$\eta_i = 10Log_{10}[\frac{1}{n}\sum\nolimits_{i=1}^{n}(\frac{\mu^2}{\sigma^2})] \quad \mu = \frac{1}{n}\sum\nolimits_{i=1}^{n} y_i^2,$$

$$\mu = \frac{1}{n-1}\sum\nolimits_{i=1}^{n}(y_i - \mu)^2 \quad (9)$$

The surface roughness and MRR that were measured using Eqs. (7) and (8), respectively, were used to estimate the S/N ratio (Table 9). Because the MRR and surface roughness had dissimilar units, they had to be rendered dimensionless for the following calculations and simultaneous optimization. Therefore, the relevant data of each output were divided according to the maximal value of the same output, and then normalized [19].

Table 10. Total normalized quality loss (TNQL) and multi S/N ratios (MSNR) for output parameters.

experiment number	simultaneous analysis of output parameters	
	TNQL	MSNR (η_i)
1	0.701321	1.54083
2	0.802734	0.95429
3	0.994312	0.02477
4	0.738774	1.31488
5	0.932901	0.30164
6	0.786452	1.04328
7	0.757271	1.20749
8	0.680715	1.67035
9	0.954625	0.20167
	Average MSNR (η_m) = 0.91769	

VII. CALCULATION OF TOTAL NORMALIZED QUALITY LOSS AND MULTISIGNAL -TO-NOISE RATIO

The total normalized quality loss (TNQL) was calculated separately in the previous section. The output parameters were weighted in this step according to the degree of importance, and then the total normalized parameters were calculated using Eq. (10). Because the surface roughness was more crucial than the MRR in this study, the weighting factor for the surface quality and MRR was set as 0.7 and 0.3, respectively. A simultaneous ratio of output was determined using Eq. (10).

$$TNQL_i = \sum wy = (0.7Ra + 0.3MRR)_i$$

$$MSNR_i = -10Log_{10}(TNQL_i) \quad (10)$$

Table 10 shows the TNQL and multisignal-to-noise ratio (MSNR).

VIII. CALCULATION OF THE MULTISIGNAL-TO-NOISE RATIO FOR EACH PARAMETER AT VARIOUS LEVELS

According to the standard array in the Taguchi method and the MSNR values calculated through the nine steps shown in Table 10, the MSNR average value for each input parameter and at various levels was measured using Eq. (11).

$$\eta_0 = \eta_m + \sum_{i=1}^{k}(\eta_i - \eta_m) \quad (11)$$

where η_i and η_m are the S/N ratio for each level and the S/N average ratio for all of the steps, respectively. The maximal amount for each input parameter was considered the optimal value. According to Table 11, the optimal case occurred with an input combination of A1B1C1D2.

Table 11. The average MSNR for each input parameter in different levels.

input parameter	average MSNR (η_0)		
	Level 03	Level 02	Level 01
voltage (A)	**1.01095**	0.82442	1.01095
pulse on time (B)	-0.56566	1.09090	**2.22782**
pulse current (C)	-0.30148	0.63546	**2.41908**
pulse off time (D)	0.71176	**1.36968**	0.20876

IX. ANALYSIS OF OPTIMUM RESULTS

To obtain a high MRR and a low surface roughness, the optimal parameter combination was A1B1C1D2; by calculating Eqs. (7) and (8), the MRR and surface roughness were equal to 7.14907 and 3.11744, respectively. Thus, the value of the surface roughness obtained using an optimal combination of input parameters was less than the minimal surface roughness obtained in the experiments, attributable to the high weighting factor (0.7) that was given to the surface roughness during value optimization. Therefore, the optimal parameters reduced the surface roughness effectively. The value of 7.14907 for the MRR can be justified in a similar manner.

X. CONCLUSION

Recent advances in material developments and a growing need for producing materials with improved properties (in addition to the extensive use of smart materials in most branches of engineering) has prompted the development of more efficient machining processes, including EDM. In this study, the values of the input parameters related to the EDM of NiTi SMA were optimized to achieve a low surface roughness and high MRR. First, nine experiments were conducted on NiTi by using brass instruments and an L9 Taguchi orthogonal array, and afterward, by achieving two output parameters (i.e., surface roughness and MRR), from these experiments, the EDM parameters were optimized. A parameter combination of A1B1C1D2 was used to achieve a low surface roughness (with a weighting factor of 0.7) and a high MRR (with a weighting factor of 0.3). Tee equations obtained using the response surface technique suggested that this method can model the surface roughness and MRR during the EDM process, and can be used to obtain the mentioned output parameters, and result in an acceptable error among considered combinations. According to the ANOVA results, the pulse current and pulse on-time were the two main and effective parameters affecting the MRR and surface roughness, respectively.

REFERENCES

1. Addington, D. M. and Schodek, D. L., *Smart Materials and New Technologies for the Architecture and Design Professions*, Harvard University, Architectural Press An imprint of Elsevier (2005).
2. Ashish, M. W., George, P. M., Raghunath, B. K., and Manocha, L. M., "EDM machining of carbon-carbon composite - a Taguchi approach," *Journal of Materials Process Technology*, Vol. 145, No. 1, pp. 66-71 (2004).
3. Daneshmand, S., Farahmand Kahrizi, E., Abedi, E., and Mir Abdolhosseini, M., "Influence of machining parameters on electro discharge machining of NiTi shape memory alloys," *Journal of Electrochemical Science*, Vol. 8, No. 3, pp. 3095-3104 (2013).
4. Douglas, C. M., *Design and Analysis of Experiments*, Wiley (2012).
5. Duerig, T., Pelton, A., and Stoeckel, D., "An overview of nitinol medical applications," *Material Science and Engineering A*, Vols. 273-275, pp. 149-160 (1999).
6. Fattouh, M., Elkhabeery, M., and Fayed, A. H., "Modelling of some response parameters in EDM," *AME Fourth Conference Military Technical College*, Cairo, Egypt (1990).
7. Hartl, D. J. and Lagoudas, D. C., "Aerospace applications of shape memory alloys," *Proceedings of the Institution of Mechanical Engineers, Part G: Journal of Aerospace Engineering*, Vol. 221, No. 4, pp. 535-552 (2007).
8. Kauffman, G. B. and Mayo, I., "The story of nitinol: The serendipitous discovery of the memory metal and its applications," *The Chemical Educator*, Vol. 2, No. 2, pp. 1-21 (1997).
9. Kneissl, A. C., Unterweger, E., and Bruncko, M., "Microstructure and properties of NiTi and CuAlNi shape memory alloys," *Journal of Metallurgy*, Vol. 11, No. 4, pp. 89-100 (2007).
10. Lan, T. S., "Virtual CNC machining and implementation of optimum MRR with tool life control," *Journal of Marine Science and Technology*, Vol. 15, No. 3, pp. 201-209 (2007).
11. Lin, C. P., Hsiao, K. M., and Wu, C. C., "Parameter analysis and optimization of electrolytic in-process dressing grinding on ceramics," *Journal of Marine Science and Technology*, Vol. 11, No. 2, pp. 104-112 (2003).
12. LotfiNeyestanak, A. A. and Daneshmand, S., "The effect of operational cutting parameters on Nitinol-60 in wire electro discharge machining," *Advances in Materials Science and Engineering*, Vol. 2013, Article ID 457186, pp. 1-6 (2013).
13. LotfiNeyestanak, A. A., Daneshmand, S., and Adib Nazari, S., "The effect of operational cutting parameters in the wire electro discharge machining (WEDM) on micro hardness of alloy surface layer," *Journal of Advanced Design and Manufacturing Technology*, Vol. 2, No. 4, pp. 51-58 (2009).
14. Morgan, N. B., "Medical shape memory alloy applications - the market and its products," *Material Science and Engineering A*, Vol. 378, pp. 16-23 (2004).
15. Panda, D. K. and Bhoi, R. K., "Artificial neural network prediction of material removal rate in electro discharge machining," *Materials and Manufacturing Processes*, Vol. 20, No. 4, pp. 645-672 (2005).
16. Patel, M. R., Barrufet, M. A., Eubank, P. T., and Dibitonto, D. D., "Theoretical models of the electrical discharge machining process. I. The anode erosion model," *Journal of Applied Physics*, Vol. 66, No. 9, pp. 4104-4111 (1989).
17. Petropoulos, G., Vaxevanidis, N. M., and Pandazaras, C., "Modeling of surface finish in electro-discharge machining based upon statistical multi-parameter analysis," *Journal of Materials Processing Technology*, Vol. 155-156, No. 30, pp. 155-156 (2004).
18. Ranjit, K. R., *A Primer on the Taguchi Method*, Society of Manufacturing Engineers, USA (2010).
19. Sabouni, H. R. and Daneshmand, S., "Investigation of the parameters of EDM process performed on smart NiTi alloy using graphite tools," *Life Science Journal*, Vol. 9, No. 4, pp. 504-510 (2012).
20. Schick, J. R., *Transformation Induced Fatigue of Ni-Rich NiTi Shape Memory Alloy Actuators*, Thesis Master of Science, Texas A&M University (2009).
21. Scott, F. M., Albert, J. S., and Qu, J., "Investigation of the spark cycle on material removal rate in wire electrical discharge machining of advanced materials," *Journal of Machine Tools and Manufacture*, Vol. 44, No. 4, pp. 391-400 (2004).